Hearing Research 283 (2012) 70–79

Contents lists available at SciVerse ScienceDirect

Hearing Research

journal homepage: www.elsevier.com/locate/heares

Research paper

Inner ear morphological correlates of ultrasonic hearing in frogs☆

Victoria S. Arch [a,b], Dwayne D. Simmons [c], Patricia M. Quiñones [d], Albert S. Feng [e], Jianping Jiang [f], Bryan L. Stuart [g], Jun-Xian Shen [h], Chris Blair [c], Peter M. Narins [b,c,*]

[a] Abbott Vascular Inc., 3200 Lakeside Drive, Santa Clara, CA 95054 2807, USA
[b] Department of Ecology and Evolutionary Biology, University of California, Los Angeles, Los Angeles, CA 90095, USA
[c] Department of Integrative Biology and Physiology, University of California, 621 Charles E. Young Drive S, Los Angeles, Los Angeles, CA 90095, USA
[d] Department of Neurobiology, David Geffen School of Medicine, University of California, Los Angeles, Los Angeles, CA 90095, USA
[e] Department of Molecular and Integrative Physiology, University of Illinois at Urbana-Champaign, Urbana, IL 61801, USA
[f] Chengdu Institute of Biology, Chinese Academy of Sciences, Sichuan 610041, China
[g] North Carolina Museum of Natural Sciences, Raleigh, NC 27601, USA
[h] State Key Laboratory of Brain and Cognitive Science, Institute of Biophysics, Chinese Academy of Sciences, Beijing 100101, China

ARTICLE INFO

Article history:
Received 28 May 2011
Received in revised form
9 November 2011
Accepted 10 November 2011
Available online 25 November 2011

ABSTRACT

Three species of anuran amphibians (*Odorrana tormota, Odorrana livida* and *Huia cavitympanum*) have recently been found to detect ultrasounds. We employed immunohistochemistry and confocal microscopy to examine several morphometrics of the inner ear of these ultrasonically sensitive species. We compared morphological data collected from the ultrasound-detecting species with data from *Rana pipiens*, a frog with a typical anuran upper cut-off frequency of ~3 kHz. In addition, we examined the ears of two species of Lao torrent frogs, *Odorrana chloronota* and *Amolops daorum*, that live in an acoustic environment approximating those of ultrasonically sensitive frogs. Our results suggest that the three ultrasound-detecting species have converged on small-scale functional modifications of the basilar papilla (BP), the high-frequency hearing organ in the frog inner ear. These modifications include: 1. reduced BP chamber volume, 2. reduced tectorial membrane mass, 3. reduced hair bundle length, and 4. reduced hair cell soma length. While none of these factors on its own could account for the US sensitivity of the inner ears of these species, the combination of these factors appears to extend their hearing bandwidth, and facilitate high-frequency/ultrasound detection. These modifications are also seen in the ears of *O. chloronota*, suggesting that this species is a candidate for high-frequency hearing sensitivity. These data form the foundation for future functional work probing the physiological bases of ultrasound detection by a non-mammalian ear.

1. Introduction

Among vertebrates, mammals are considered high-frequency hearing specialists (Heffner and Heffner, 2007). The majority of mammalian species hears well into the ultrasonic range (i.e., >20 kHz) while other vertebrates possess comparatively limited sensitivity (Heffner and Heffner, 1998; Fettiplace and Fuchs, 1999; Dooling et al., 2000, but see Mann et al., 2001). Anuran amphibians (frogs and toads) are among the taxa that have been considered to possess restricted high-frequency hearing ability, with an upper detection limit of 5–8 kHz (Loftus-Hills and Johnstone, 1970). However, this assumption has been challenged by the recent discovery of three frog species that detect ultrasound: *Odorrana tormota*, *Odorrana livida* and *Huia cavitympanum* (upper hearing limits of 34, 22 and 38 kHz, respectively). Two of these species, *O. tormota* and *Huia cavitympanum,* have been demonstrated to

Abbreviations: AEP, auditory evoked potentials; AP, amphibian papilla; BL, bundle length; BP, basilar papilla; ESA, epithelium surface area; HCC, hair cell count; BP REA, basilar papilla recess entrance area; RT, room temperature; SL, soma length; SVL, snout-vent length; TM, tectorial membrane.

☆ Support information: Financial support was provided by a National Science Foundation Doctoral Dissertation Improvement Grant (no. 0806207) to VSA, grants from the National Institute on Deafness and Other Communication Disorders to DDS (no. DC004086) and PMN (no. DC00222), the Paul S. Veneklasen Research Foundation to PMN, the National Science Foundation (CRCNS-0422073) to ASF, and the National Natural Science Foundation of China to JPJ (no. 31071906) and JXS (no. 30730029).

* Corresponding author. Department of Integrative Biology and Physiology, University of California, 621 Charles E. Young Drive S, Los Angeles, Los Angeles, CA 90095, USA. Tel.: +1 310 825 0265; fax: +1 310 206 3987.
E-mail address: pnarins@ucla.edu (P.M. Narins).

0378-5955/$ – see front matter © 2011 Elsevier B.V. All rights reserved.
doi:10.1016/j.heares.2011.11.006

communicate ultrasonically (Feng et al., 2006; Arch et al., 2009). The *Odorrana* and *Huia* genera are from distinct evolutionary lineages (Stuart, 2008) suggesting that the frogs converged on the ability to detect extraordinarily high frequencies. All three species are torrent frogs; they inhabit rapid-flowing hill or mountain streams, and call alongside rushing water that produces an abundance of broadband, predominately low-frequency, background noise (Feng et al., 2002; Narins et al., 2004; Arch et al., 2008). The convergence of *O. tormota* and *H. cavitympanum* on ultrasonic communication may have resulted from parallel selection pressure to place acoustic signals within relatively noise-free windows of their environments' ambient spectra (Narins et al., 2004; Arch et al., 2008).

The inner ear mechanisms subserving exceptional high-frequency hearing in frogs are unknown. In mammals, the advent of high-frequency sensitivity is attributed to key morphological innovations within the ear, including the extension of a flexible, mechanically tuned membrane on which the sensory receptors sit (i.e., the basilar membrane), and the specialization of inner ear supporting and sensory cell types (Fettiplace and Fuchs, 1999). These features are not present in frogs.

The anuran inner ear is unique among vertebrates in its possession of two dedicated auditory endorgans, the amphibian papilla (AP) and the basilar papilla (BP) (Wever, 1973; Baird, 1974; Capranica, 1976; Lombard and Bolt, 1979; Lewis et al., 1992). Each lies within its own chamber and is sensitive to a distinct band of frequencies. The AP responds to low and middle frequencies and is tonotopically organized, with low-frequency-sensitive hair cells located rostrally and mid-frequency cells located caudally (Lewis et al., 1982a, 1982b). The BP is a simpler organ that acts as a mechanical resonator, responding to a restricted, higher-frequency band (Feng et al., 1975; Lewis et al., 1982a, 1982b; Megela and Capranica, 1982; Wilczynski and Capranica, 1984; Ronken, 1990; van Dijk and Manley, 2001; Meenderink et al., 2005). Mechanotransduction in the ear is performed by hair cells, which are common to all vertebrates. However, unlike most amniote hair cells, those of the auditory epithelia in anurans are firmly attached to the walls of the organ chambers (Lewis et al., 1982a). As a result, acoustic stimuli are not filtered by graded mechanical properties of an underlying basilar membrane prior to hair cell transduction. Hence, extrinsic tuning of the stimulus preceding transduction is restricted to the motion of an overlying tectorial structure in which the hair cell ciliary bundles are embedded (Shofner and Feng, 1983; Hillery and Narins, 1984). Additional tuning in the frog ear depends on intrinsic properties of the hair cells themselves, including ciliary mechanical coupling and ion channel kinetics (Pitchford and Ashmore, 1987; Simmons et al., 1994; Smotherman and Narins, 1999a, b).

Across vertebrate taxa, intrinsic hair cell tuning is related to morphological properties of the hair cell soma and bundle. Soma lengths of mammalian outer hair cells (Bohne and Carr, 1985; Fettiplace and Fuchs, 1999), goldfish saccular hair cells (Sugihara and Furukawa, 1989) and frog AP hair cells (Simmons et al., 1994) decrease systematically with increasing frequency sensitivity along the auditory organ's tonotopic axis. Experiments with isolated frog AP hair cells demonstrate that whole-cell capacitances vary predictably with soma length, providing additional evidence that the hair cell's resonant frequency is inversely related to its length (Smotherman and Narins, 1999a, b). Bundle heights also negatively correlate with the frequency of maximal hair cell sensitivity in the mammalian cochlea (Lim, 1980; Fettiplace and Fuchs, 1999), and chick (Tilney and Saunders, 1983) and lizard basilar papillae (Mulroy, 1974; Turner et al., 1981).

To gain a greater understanding of the extrinsic and intrinsic mechanisms subserving high-frequency hearing in the frog inner ear, we used immunohistochemistry and confocal microscopy to examine the auditory organ morphology of *O. tormota, O. livida* and *H. cavitympanum*. We investigated features of the auditory papillae such as papillar surface area and number of hair cells, as well as hair-cell-specific morphometrics, including soma and bundle lengths. This investigation allowed us to test the hypothesis that the ultrasonically-sensitive frogs' inner ears had undergone a major reorganization to enable ultrasound reception, and to examine smaller-scale functional modifications that may play key roles in high-frequency detection. We compared the inner ear features of *O. tormota, O. livida* and *H. cavitympanum* with one another, and with those of the leopard frog (*Rana pipiens)*, which has a typical anuran hearing range (upper cut-off frequency of ~ 3 kHz). We additionally examined the inner ears of two sympatric species of torrent frogs in Laos – *Odorrana chloronota* and *Amolops daorum* - which call in an environment with an ambient noise spectrum that is very similar to those of the ultrasound-sensitive species. As yet, there are no behavioral data indicating whether these frogs hear or communicate using ultrasound. Our comparative analysis provides a context within which to evaluate the species' auditory apparatus and form hypotheses about their auditory sensitivity.

2. Materials and methods

2.1. Specimen collection

We collected sexually mature *O. tormota* males by hand from their natural calling sites along the banks of the Tau Hua Creek, Anhui, China (30°06′N, 118°10′E), from 9 to 11 May, 2010. We obtained *O. livida* males in the same manner from their calling sites in Hongyuan Gou, Sichuan, China (28°38′N, 106°18′E), from 30 May – 5 June, 2010. We collected both species between approximately 1900–2230 h.

We found *H. cavitympanum* males along the banks of the Nyipa River in Gunung Mulu National Park, Sarawak, Malaysia (04°03′N; 114°51′E). We collected the frogs as part of a separate research project and preserved their ear tissues after the project's completion. Additional details are presented in Arch et al. (2009).

We collected males of *O. chloronota* and *A. daorum* in the vicinity of the Tad Loi Waterfall in the Phou Louey National Protected Area, Viengthong District, Huaphahn Province, Laos (20.23°N 103.21°E), on 13–18 March, 2009. We found the frogs between 1900 and 2230 h at approximately 1200 m elevation. After sacrificing the frogs (see below), we removed their heads and preserved the bodies as voucher specimens at the Field Museum of Natural History (*O. chloronota*: BLS12978, BLS13047, BLS13048, BLS13049, BLS13095; *A. daorum*: BLS13044, BLS13058, BLS13059).

Rana pipiens were purchased from a commercial supplier and housed in UCLA vivarium facilities.

To sacrifice the frogs, we first deeply anaesthetized them by liberally applying topical anesthetic (*R. pipiens*, *O. tormota*, *O. livida*; Benzocaine, 7.5%; Del Pharmaceuticals, Inc., Uniondale, NY), or by immersing them in a solution of tricaine methanesulphonate [0.3% solution for *H. cavitympanum*; an effective but unknown concentration (prepared upon collection in the field) for *O. chloronota* and *A. daorum;* MS-222; Sigma, Saint Louis, MO], followed by swift decapitation.

All animal care adhered to the ABS Guidelines for the use of animals in research and was approved by the UCLA Animal Research Committee (Protocol # 094-086-51).

2.2. Tissue preparation

We removed the lower jaw and opened the otic capsules ventrally, via the roof of the mouth, to expose the inner ear

membranous labyrinth. We then made a small opening in the labyrinth using fine forceps and dripped a freshly prepared solution of 4% paraformaldehyde (Ted Pella, Redding, CA) in phosphate buffer with frog-specific osmolarity (e.g., frog-specific phosphate buffered saline; FPBS) into the inner ears to insure that the sensory epithelia came into immediate contact with the fixative. Following this procedure, we immersed the entire head in the fixative solution and gently agitated it at room temperature (RT) for 2 h. We then rinsed the tissues in FPBS and, when possible, stored them at 4 °C. We kept the heads collected in the field in China at ambient temperature until there was access to refrigeration (~2–7 days). We stored the *H. cavitympanum* tissues in fixative at 4 °C for approximately 4 months, and then in FPBS for an additional *ca.* 6 months at 4 °C before using them in the present study.

2.3. Immunohistochemistry

We removed the inner ears from the chemically fixed heads and dissected them down to the auditory organs while maintaining immersion in FPBS. We kept the surgically isolated BPs intact since the hair cell array is unobscured in the intact form. To expose the AP sensory epithelium, we cut off the ventral wall of the organ with microdissection scissors and removed the tectorial membrane using fine forceps. We placed the organs in a well plate and bathed them in 1% Triton X-100 in FPBS for 30 min to enhance their permeability; the tissues were gently agitated through this period and during the subsequent steps. We rinsed the organs 4 × 15 min in FPBS and soaked them for 1 h in a blocking solution to minimize non-specific antigen binding. The blocking solution consisted of 5% normal donkey serum (NDS) and 0.05% bovine serum albumin (BSA; Sigma) in a low-calcium buffer (BSA-block), and was used for all succeeding dilutions. We immediately followed blocking with an overnight incubation at RT in monoclonal rabbit antibody against Myosin VI (1:500; Proteus Biosciences 25-6791; Ramona, CA) to label hair cell somata. The next morning, we rinsed the tissues [4 × 15 min in 0.1% Tween in FPBS (TwFPBS)] and incubated them for 2 h in the secondary antibody Alexa Fluor 594 donkey anti-rabbit IgG (1:200; Invitrogen A21207, Carlsbad, CA). We then rinsed the tissues again (4 × 15 min in TwFPBS) and incubated them for another 2 h in a cocktail containing phalloidin conjugated to Alexa-Fluor 488 (1:100; Invitrogen A12379) and the nucleic acid stain, DAPI (1:1000; Thermo Fisher Scientific 46190, Waltham, MA). Phalloidin binds to filamentous actin which forms of the core of stereocilia, therefore it selectively labels hair cell bundles. After a final rinse (4 × 15 min in FPBS), we whole-mounted the tissues on glass coverslips using Mount-Quick aqueous mounting medium (Thermo Fisher Scientific). Basilar papillae were mounted directly between two coverslips. Amphibian papillae were mounted using a Secure-Seal spacer (Invitrogen) between two coverslips to ensure that the 3-dimensional structure of the organ remained intact. After drying for 24 h, we attached the mounted tissues to Superfrost Plus slides (Thermo Fisher Scientific) using double-sided tape; this process allowed the tissues to be rotated and/or turned over if necessary for better imaging results.

2.4. Confocal microscopy and data analysis

Labeled organs were imaged with a confocal microscope (Zeiss LSM 5) attached to an upright microscope (Zeiss, AxioImager) using Zen Software (Carl Zeiss MicroImaging Inc., Thornwood, NY). This confocal microscope is equipped with single-photon (Argon (488, 514 nm), HeNe (543 nm) and Red Diode (633 nm)) lasers. The same acquisition parameters were used for all control and experimental scans. The epithelia were first scanned in their entirety using a low-powered (10×) dry objective (Fig. 1A). Subsequently, we took a single high-powered image with a 63× water immersion Plan Achromat objective from the BP and three high-powered images from each AP. We captured the AP 63× images from the organ's rostral end, middle (approximately at the position of the tectorial curtain; Lewis and Li, 1975; Lewis, 1976) and caudal extension. We verified the locations of the AP high-powered scans by taking a subsequent 10× image using a single laser line; photobleaching of the fluorescent labels during the high-magnification scans allowed us to determine their positions precisely (Fig. 1B).

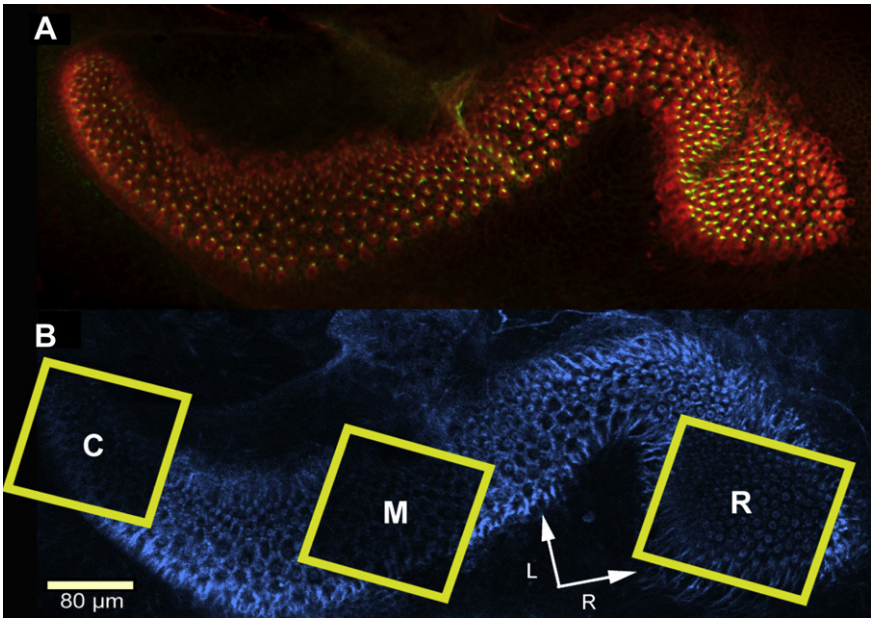

Fig. 1. A: Scanning confocal image stack (projected onto a 2D plane) of the amphibian papilla of *O. chloronota*. The image was captured with a 10× objective. Hair cell somata appear red (530 nm laser line), and hair bundles appear green (480 nm laser line). B: The same amphibian papilla after high-powered (63×) scans have been taken from the rostral (R), middle (M) and caudal (C) regions of the epithelium. Photobleaching causes the epithelium to appear dim in the regions of the high-powered scans. The tissue is being illuminated by the 633 nm laser line. L, lateral. (For interpretation of the references to colour in this figure legend, the reader is referred to the web version of this article.)

Image processing was performed with Volocity Visualization (Improvision, Perkin–Elmer, Coventry, England) software, a 3D-image analysis program. All measurements were all taken by the same person, who was unfamiliar with the hypothesis of the experiment. We collected data from the confocal image stacks using the measurement module of Volocity. Our measurement data from 10× images included epithelium surface area (ESA) and hair cell count (HCC). ESA was determined by Volocity from a line drawn manually around the perimeter of the epithelium. We counted the hair cells by using the "point" tool to label each cell manually (Fig. 2). As a proxy for the size of the BP organ, we measured the basilar papillar recess entrance area (REA; see *Discussion*; Fig. 2). The data we collected from the 63× images included hair cell soma length (SL) and bundle length (BL). We measured soma length from the mid-point of the bundle base to the soma base, through the center of the nucleus. The hair cell nuclei were not labeled by the antibody against Myosin VI so they appeared as voids in the fluorescently labeled cell bodies. We measured bundle length from the mid-point of the bundle base to the tip of the tallest stereocilium. We measured all cells and bundles from which measurements could be taken unambiguously. Due to the orientation of the whole-mounted tissues, we were able to collect AP SLs predominately along the periphery of the organ. Our measurements of hair cell SLs were restricted to cells in the peripheral regions of the rostral, middle and caudal portions of the AP where the full soma was visible/measurable, whereas BLs measurements were taken from cells throughout these regions of the frog's AP.

We exported the resulting morphometric data to Excel for sorting and analysis. We pooled data from the left and right ear of a single frog since we did not consider these data to be independent. We used both SPSS (SPSS Inc., Chicago, IL.) and the R computer package (2004) to test for differences among the species' means for each measured parameter using univariate ANOVA, and performed pair-wise comparisons with Tukey's post-hoc test.

3. Results

We did not correct our morphological measurements for shrinkage caused by chemical fixation of the tissues. The inner ear is comprised of a complex mixture of tissue types including

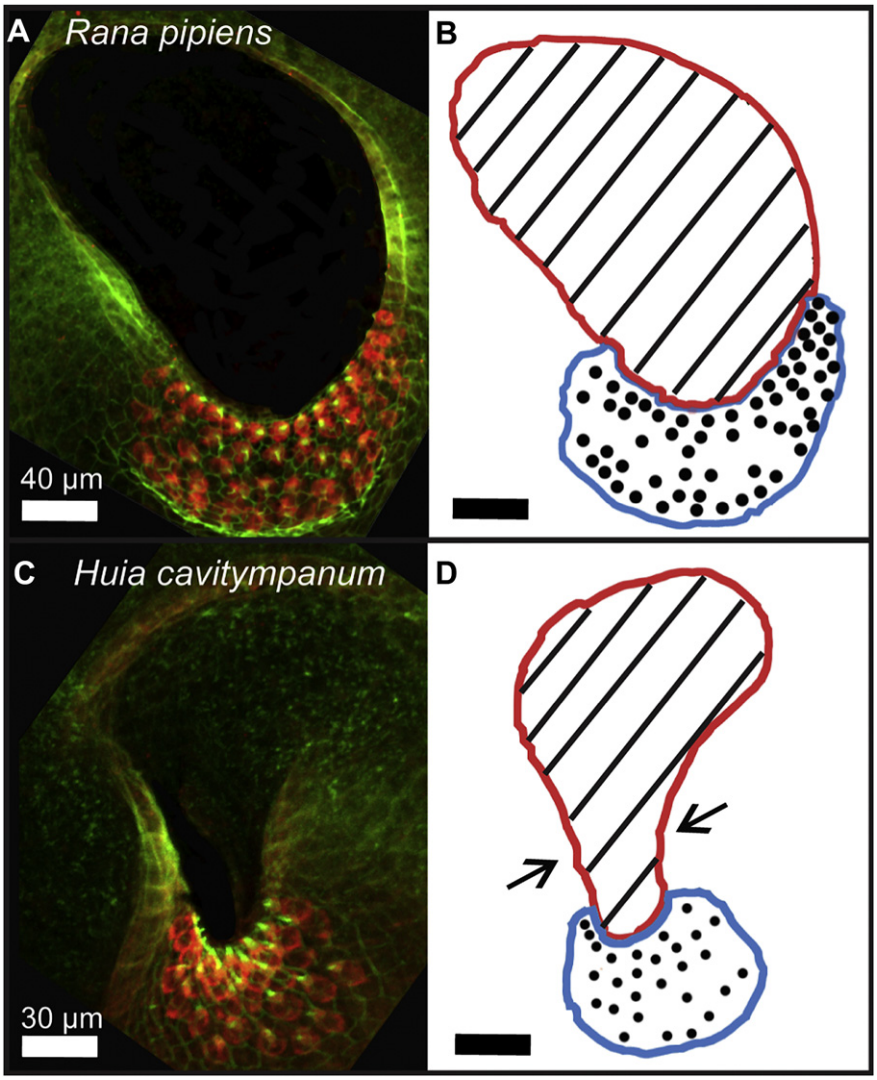

Fig. 2. Scanning confocal image stacks (projected onto a 2D plane) of the A: *Rana pipiens* and C: *Huia cavitympanum* basilar papillae. Images were captured with a 10× objective. Hair cell somata appear red (530 nm laser line), and hair bundles appear green (480 nm laser line). B: and D: Schematics illustrating the measurement data collected from the basilar papillae. Black lines: area of recess entrance (red lines indicate recess perimeter); Blue: epithelium surface boundary; Black points: individual hair cells. Arrows in D indicate approximate points of pronounced narrowing of the *H. cavitympanum* papillar recess. (For interpretation of the references to colour in this figure legend, the reader is referred to the web version of this article.)

cartilaginous, epithelial, neural and gelatinous structures and the amount of shrinkage can be expected to differ amongst the various tissue types. However, gross inner-ear morphology was consistent among the frogs we examined; thus, there is no evidence for interspecific differences in histology in the tissues of interest. As a result, we assume that differential shrinkage between species was minimal, and its effect on relative dimensions insufficient to influence the overall conclusions drawn from the data. We found significant differences in the means of all morphological variables across all species studied (the results of the ANOVAS including F- and *P*-values are provided in Table 1, Supplemental Materials). More specifically, we were interested in which species showed significant differences among the suite of morphological variables tested.

3.1. Amphibian papilla

We measured hair cell SLs (from the periphery) and BLs from the rostral, middle and caudal regions of the frog's AP. These sampling locations span the presumed tonotopic axis of the organ (Lewis et al., 1982a, 1982b; Simmons et al., 1994). In accord with the results of Simmons et al. (1994), SL decreased from the organ's rostral (low-frequency sensitive region) to caudal (mid-frequency sensitive region) end in all six species (Fig. 3A–C). We found the same trend in our BL measurements (Fig. 3D–F) in all but one species; in *R. pipiens* the BL values increased slightly from the rostral to middle AP (Fig. 3D, E). These results suggest that, other than *R. pipiens*, inverse relationships exist between both the hair cells' SL and BL, and the frequency to which the cells are tuned.

Soma length values followed the same overall trend in all three AP regions. *R. pipiens* and *A. daorum* had the longest SL, and *H. cavitympanum* and *O. chloronota* had intermediate values. *O. tormota* and *O. livida* SL were the smallest (Fig. 3A–C). Statistically significant groupings varied slightly in each AP region, however. For the rostral AP, the SL values of *R. pipiens* and *A. daorum* were significantly greater than that of *O. livida*, and the SL of *A. daorum* was greater than *O. tormota*. The SL values of *H. cavitympanum* and *O. chloronota* were intermediate and did not differ significantly from any other species (Fig. 3A). In the middle AP, the SL values of *H. cavitympanum* and *O. chloronota* were smaller than those of *R. pipiens* and *A. daorum*, and were greater than those of *O. tormota* and *O. livida* (Fig. 3B), but these differences were not statistically significant. For the caudal AP, the SL value of *H. cavitympanum* only differed significantly from that of *O. tormota*, which had a significantly smaller SL value than all species except *O. livida*. The SL value of *O. chloronota* was intermediate, and did not differ significantly from any other species (Fig. 3C).

Bundle length only differed significantly between *O. livida* and *O. chloronota* in the rostral AP (Fig. 3D). However, in the middle AP, the differences between the species' BL values became more pronounced: *R. pipiens* and *A. daorum* had significantly greater BL values than those of all three ultrasonically sensitive frogs, and *O. chloronota* was intermediate (Fig. 3D). In the caudal region, *R. pipiens* and *A. daorum* BLs were greater than that of all other species (Fig. 3E, F).

The AP ESA and HCC scaled approximately with the average body size of the species ($r^2 = 0.83$ and 0.74, respectively; Fig. 4D, E).

3.2. Basilar papilla

Unlike the AP, the ESA and HCC of the BP scaled much less allometrically with the species' average body size as reflected in the lower correlation coefficients ($r^2 = 0.28$, $P = 0.277$; and 0.45, $P = 0.148$, respectively; Fig. 4B, C). The same was true for BP REA, our proxy for BP organ size ($r^2 = 0.58$, $P = 0.078$; Fig. 4A). *Rana pipiens* had values for these metrics that were significantly greater than all other species ($P < 0.05$; Fig. 5A–C). The trends in the data suggest that *A. daorum* also had larger values for these metrics than the ultrasonically sensitive species and *O. chloronota*, although the small sample size for *A. daorum* precluded some of these differences from being statistically significant. The three ultrasound-detecting frogs had values for these metrics that were statistically indistinguishable from one another and from *O. chloronota* (Fig. 5A–C). These data indicate that *H. cavitympanum*, *O. tormota*, *O. livida* and *O. chloronota* have significantly smaller BP organs and sensory epithelia than those of *R. pipiens* and *A. daorum* (*P* values for all sixteen comparisons <0.0001).

Basilar papilla SL and BL values from the ultrasonically sensitive frogs and *O. chloronota* were not significantly different and their SL values were significantly smaller than those of *R. pipiens* and *A. daorum*. The same pattern was seen in the BL values with the exception that the BL of *O. chloronota* was not statistically different from that of *A. daorum* (Fig. 5D, E).

4. Discussion

This study comprises a quantitative investigation of the auditory organs in the inner ears of *H. cavitympanum*, *O. tormota* and

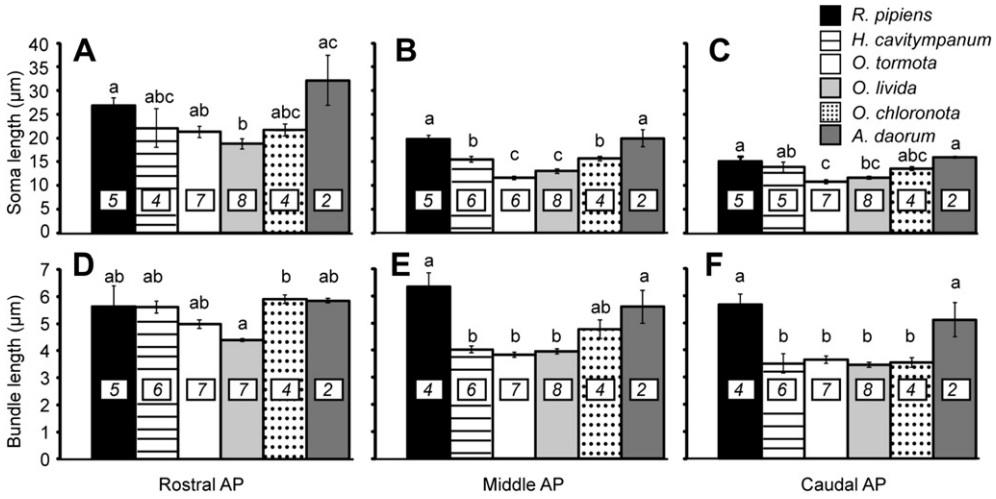

Fig. 3. Soma and bundle lengths from the rostral (A and D), middle (B and E) and caudal (C and F) regions of the species' APs. Numbers indicate sample sizes. Letters denote statistically significant differences in pairwise comparisons using Tukey's post-hoc analysis with $\alpha = 0.05$. If a pair of species shares a common letter, they are *not* significantly different in that trait.

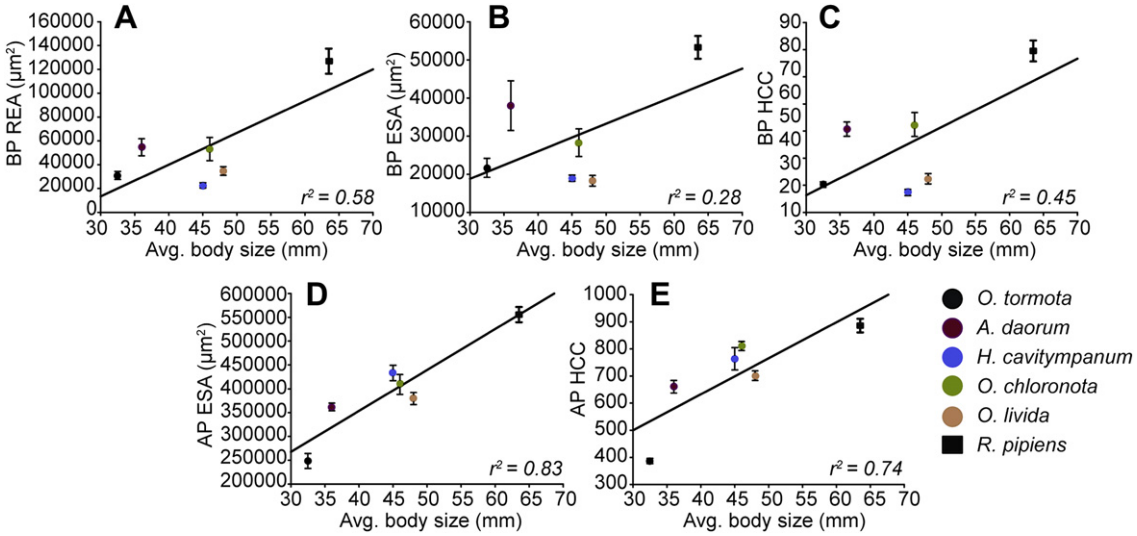

Fig. 4. A: Recess entrance area (REA) of the basilar papilla; epithelium surface area (ESA) of the B: basilar papilla and D: amphibian papilla and hair cell count (HCC) of the (C) basilar papilla and (E) amphibian papilla plotted against the average body size of the species. Solid lines indicate the best fit regressions. Data points represent means and standard errors.

O. livida, the first amphibians found to detect ultrasonic frequencies (Feng et al., 2006; Arch et al., 2009). To date, these are the only frogs known to detect frequencies above a previously postulated upper sensitivity limit of ~5–8 kHz for the taxon (Loftus-Hills and Johnstone, 1970). Therefore, we hypothesized that the inner ears of these species have undergone a radical reorganization of their inner ears to facilitate their extended sensitivity. Our observations, however, clearly indicate that this is not the case; the layout and gross structural features of the species' auditory organs are consistent with those of frogs that lack high-frequency sensitivity. These observations suggest an alternate hypothesis: that a mosaic of smaller modifications within frogs' inner ears might facilitate high-frequency sensitivity. We have enumerated these modifications which include: 1. reduced BP chamber volume, 2. reduced tectorial membrane mass, 3. reduced hair bundle length, and 4. reduced hair cell soma length. While none of these factors on its own could account for the US sensitivity of the inner ears of these species, the combination of these factors appears to extend their hearing bandwidth, and facilitate high-frequency/ultrasound detection.

4.1. Comparison between ultrasound-sensitive and control inner ears

Our results reveal interesting morphological differences between the auditory epithelia of the ultrasound-sensitive species and those of *R. pipiens*. The frequency ranges to which the ultrasound-detecting frogs' auditory organs are sensitive are currently unknown. Therefore, interpreting the significance of our morphological data necessitates formulating preliminary hypotheses about the distribution of frequency sensitivity between these organs. In *R. pipiens*, the AP transduces frequencies from *ca.* 100–1250 Hz and the BP is tuned to ~2 kHz (Feng and Shofner, 1981; Ronken, 1990). Thus, *R. pipiens* auditory sensitivity spans *ca.* 1900 Hz. Although none of the ultrasonic frogs' frequency sensitivity has been measured electrophysiologically below 1 kHz, tympanic membrane vibration data from the species indicate that their eardrums vibrate in response to frequencies as low as 200 Hz (Gridi-Papp et al., 2008; Arch et al., 2009; Gridi-Papp, unpublished data). These results suggest that the low-frequency detection ability of these species is consistent with other frogs tested to date

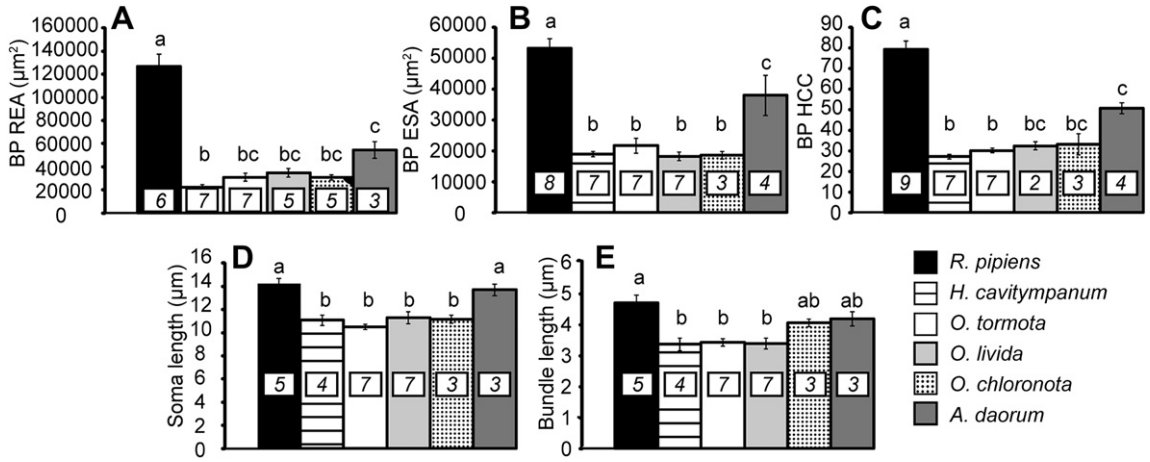

Fig. 5. Morphometric data from the basilar papilla. A: Recess entrance area (REA); B: Epithelium surface area (ESA); C: Hair cell count (HCC); D: Hair cell soma length; E: Hair cell bundle length. Numbers indicate sample sizes. Letters denote statistically significant differences in pairwise comparisons using Tukey's post-hoc analysis with $\alpha = 0.05$. If a pair of species shares a common letter, they are *not* significantly different in that trait.

(*ca*. 100–200 Hz) (Feng et al., 1975; Lewis et al., 1982a; Narins and Hillery, 1983; Hillery and Narins, 1987). Under this assumption, *H. cavitympanum*, *O. tormota* and *O. livida* auditory sensitivity spans *ca*. 37,800 Hz, 33,800 Hz and 21,800 Hz respectively, and therefore the species display a substantially broader sensitivity bandwidth than that of *R. pipiens*. Across frog species, the BP is consistently tuned to a species-specific band of frequencies (Wilczynski and Capranica, 1984; Ronken, 1990). Auditory-evoked potentials (AEP) recorded from the central auditory system of *H. cavitympanum* and *O. tormota* show a high-frequency sensitivity peak at *ca*. 25 kHz (Arch et al., 2009) and *ca*. 20 kHz (Feng et al., 2006), respectively. Since the BP is the high-frequency detection organ of anurans, these data suggest that BP is likely responsible for transducing ultrasounds. A high-frequency peak is less apparent in the AEP recordings from *O. livida* (Feng et al., 2006) but given that *O. tormota* and *O. livida* are congeneric, and the species display a remarkable convergence in auditory organ morphometrics (see below), we hypothesize that the *O. livida* BP is similarly responsible for high-frequency/ultrasound transduction. Lower-frequency sensitivity peaks at *ca*. 8 and 12 kHz in the AEP audiogram of *H. cavitympanum* (Arch et al., 2009), and a sensitivity plateau below *ca*. 10 kHz in *O. tormota* (Feng et al., 2006) are presumed to originate from the AP. Based on this hypothesized distribution of frequency sensitivity between the *H. cavitympanum* and *O. tormota* auditory organs, we suggest that the ultrasonic frogs' BPs are sensitive to substantially higher frequencies than that of *R. pipiens* and that their APs are sensitive to a wider bandwidth of frequencies (i.e., *H. cavitympanum*: ~200 Hz - ≥12,000 Hz; *O. tormota*: ~200 Hz - 10,000 Hz; *R. pipiens*: ~100 Hz–1250 Hz). Direct tests of these inferences, and a more detailed examination of the frequency sensitivity of the *O. livida* peripheral and central auditory system, are planned in future studies.

4.2. The basilar papilla

The sensory epithelium of the frog BP is located at the base of a tubular outpocket of the sacculus, an inner-ear endorgan primarily responsible for detecting substrate vibrations (Narins, 1990; Yu et al., 1991). A tectorial membrane (TM) spans the lumen of the papillar recess, connecting to the stereociliary bundles of the sensory hair cells that are embedded in the recess's cartilaginous wall (Wever, 1985). The tuning curves of BP nerve fibers within a particular animal have nearly identical shapes and characteristic frequencies (Ronken, 1990; van Dijk and Meenderink, 2006). Therefore, the BP is believed to act as a single tuned, mechanical resonator (Capranica and Moffat, 1977; Ronken, 1990; van Dijk and Manley, 2001; Meenderink et al., 2005).

Mechanical tuning of the BP presumably results from a combination of anatomical features, including the large-scale fluid dynamics of the inner ear and the frequency tuning of the contact membrane (Purgue and Narins, 2000a, 2000b). These features influence the movement of the TM which interacts directly with the hair cells. Recently, Schoffelen et al. (2009) optically measured the mechanical response of the BP TM in *R. pipiens* and found that it is tuned to 2 kHz, corresponding closely to the characteristic frequencies of the species' BP nerve fibers. These data suggest that TM movement may be primarily responsible for the frequency selectivity of the organ (Schoffelen et al., 2009).

Tectorial membrane tuning is influenced strongly by its interaction with the lumen boundary. In fact, it has been suggested that mechanical coupling between the TM and stereociliary bundles acts as a local resonance system (Zwislocki, 1980a, 1980b; Lewis and Leverenz, 1983) with a resonance frequency that is directly proportional to the resonator's stiffness (for additional detail, see Shofner and Feng, 1984). Our hypothesis that the ultrasonically sensitive frogs' BPs transduce ultrasounds suggests that they have a substantially higher resonance frequency, and thus greater stiffness, than the *R. pipiens* BP. A key factor in the stiffness of the system is the stereocilia, which are rigid structures (Flock, 1977, 1982; Strelioff and Flock, 1982). Bundle stiffness is inversely correlated with stereociliary height (Flock, 1982; Strelioff and Flock, 1982; Authier and Manley, 1995) and directly correlated with stereocilia number (Authier and Manley, 1995; Fettiplace and Fuchs, 1999). The latter two factors typically covary: a reduction in bundle height is accompanied by an increase in the number of stereocilia per bundle (Tilney and Saunders, 1983; Hackney et al., 1993; Köppl and Authier, 1995). Our data indicate that the ultrasonic frogs' BP hair bundles are, on average, ~1.3 μm (~30%) shorter than those of *R. pipiens* (means: BL_{Hc} = 3.31 μm, BL_{Rp} = 4.75 μm, Fig. 5E). These shorter stereocilia will be comparatively stiffer, increasing the system's resonant frequency. As a comparison, the mean bundle lengths for basal (high-frequency) inner hair cells from several mammals sensitive to ultrasound, and the upper frequency limit of their hearing are: chinchilla: BL = 1.75 μm, upper limit: 25 kHz; rat: BL = 2.3 μm, upper limit: 59 kHz; bat: 2.5 μm, upper limit: 100 kHz (Echteler et al., 1994). From our confocal images, we were unable to determine the number of stereocilia per bundle; future studies employing electron microscopy will be necessary for this assessment.

Along with increased stereociliary stiffness, a decrease in the resonator mass of the ultrasonic frogs' BPs could also play a significant role in increasing their resonance frequencies (for additional detail, see Shofner and Feng, 1984). The mass term affecting the local resonance frequency of the coupled TM and sensory epithelium is primarily determined by the mass loading of the TM on the stereocilia (Zwislocki, 1980a, 1980b). We did not measure TM mass in this study; however, our data indicate that the ultrasonic frogs' BP REAs, a proxy for the organ's size, are approximately 18% (*H. cavitympanum*), 24% (*O. tormota*) and 27% (*O. livida*) that of *R. pipiens* (Fig. 5A). The average body size [snout-vent length (SVL)] of the ultrasound-detecting species is 71% (*H. cavitympanum*), 51% (*O. tormota*) and 76% (*O. livida*) that of the *R. pipiens* used in our study [*H. cavitympanum* avg. SVL = 45 mm (Yang, 1991); *O. tormota* avg. SVL = 32.5 mm (Fei, 1999); *O. livida* avg. SVL = 48 mm (Fei, 1999); *R. pipiens* avg. SVL = 63.5 mm (Arch, personal obs.)] hence the considerable size difference between the species' BPs is not solely due to allometric scaling (Fig. 4A). In a study of developing auditory organs in the frog, smaller tectorial membrane volume, and thus mass, has been shown to be correlated with decreased BP chamber volume (Shofner and Feng, 1984). This suggests that the substantially reduced size of the ultrasound-sensitive frogs' BPs will correlate with a significantly less-massive TM. Furthermore, qualitative observations of our image stacks indicate that the *H. cavitympanum, O. tormota* and *O. livida* BP chambers narrow adjacent to the sensory surface (e.g. Fig. 2 D). This narrowing results in a smaller area over which the TM must stretch to cover the sensory epithelium. In sum, we conclude that a possible explanation for the substantially reduced size of the ultrasound-sensitive frogs' BPs is that it permits a markedly smaller TM; this smaller, and therefore lighter TM decreases the mass loading of the BP resonance system, increasing the organ's resonance frequency.

Our SL data from the BP suggest another way that the ultrasound-detecting ear is specialized to transduce high frequencies. The average BP SL of ultrasonically sensitive frogs is ~3–4 μm shorter than in *R. pipiens* (Fig. 5D). A negative relationship between hair cell SL and frequency sensitivity has been demonstrated across vertebrate classes, including the frog AP (Simmons et al., 1994), the chick basilar papilla (Fuchs et al., 1988) and the mammalian cochlea (Wada, 1923; Iurato, 1967; Bohne and Carr, 1985). The time constant of the hair cell membrane largely determines how quickly the

membrane can charge and discharge, and thus defines the maximum frequencies the cell can encode. Whole-cell capacitances of frog AP and saccular hair cells have been shown to correlate directly with cell SL (Smotherman and Narins, 1998, 1999b). Assuming this relationship holds in the BP and that variation in membrane resistance is low (Smotherman and Narins, 1999a), the shorter hair cells of *H. cavitympanum, O. tormota* and *O. livida* are predicted to have a shorter membrane time constant and thus faster dynamics than those of *R. pipiens*, consistent with their role in transducing higher frequencies.

Taken together, the highly convergent morphological data collected from the BPs of the frogs that detect ultrasounds suggest that this organ appears specialized for transducing high-frequency sounds. Shorter hair bundle length and smaller organ size imply that the TM-sensory epithelium coupling in these frogs is substantially stiffer than in *R. pipiens*. Additional potential contributions to BP tuning of larger scale factors like inner-ear fluid dynamics and contact membrane will be of interest in future studies.

4.3. The amphibian papilla

The AP is the larger and more complex of the two inner-ear organs in frogs (Geisler et al., 1964; Wever, 1973) and lies in a medial extension of the sacculus. Our data indicate that the tested species' AP ESA and HCC scale approximately allometrically with average body size (Fig. 4D, E). This is in contrast to the BP, which has significantly smaller ESA and HCC values in ultrasound-sensitive frogs relative to body size (Fig. 4B, C). Thus, if our hypothesis of AP frequency sensitivity bandwidth is correct, the broader bandwidth of the ultrasound-detecting frogs' APs appears to be independent of epithelium size or cell number. Our data also indicate no significant difference in BL between the species in the rostral AP (Fig. 3A). Soma length in this region only differs significantly between *R. pipiens* and *O. livida*. These data suggest that mechanical tuning related to hair cell structural composition is comparable between *H. cavitympanum*, *O. tormota* and *R. pipiens* in this AP region. This result agrees with our inference that the frogs have similar low-frequency hearing limits, although a thorough test of this prediction requires electrophysiological exploration of *H. cavitympanum* and *O. tormota* low-frequency hearing. In the middle portion of the AP the ultrasound-sensitive frogs' SL and BL are significantly shorter than in *R. pipiens* (Fig. 3B). A similar pattern is seen in the BL data from the caudal AP; however there is no difference between *H. cavitympanum* and *R. pipiens* SL in this region (Fig. 3C). As in the BP, shorter hair cells in the middle region of the ultrasound-detecting frogs' AP are expected to have a smaller capacitance and thus shorter membrane time constant, allowing the encoding of higher frequencies. This conclusion is in agreement with our expectation that these frogs' AP transduction range covers a wider high-frequency bandwidth than that of *R. pipiens*.

As in the basilar papilla, the absence of a flexible membrane underlying the AP sensory epithelium restricts extrinsic hair cell tuning to the coupling between the hair bundles and the overlying TM. If we again consider this coupled system as a resonator (Lewis and Leverenz, 1983; Zwislocki, 1980a, 1980b) with stiffness, and thus resonant frequency, inversely related to bundle length (Shofner and Feng, 1981), our BL data indicate an increased resonant frequency of the ultrasound-detecting frogs' AP relative to *R. pipiens* as we move away from the rostral patch along the tonotopic axis (Fig. 5D, E). This provides additional support for our hypothesis that these frogs' APs transduce an extended range of frequencies that includes substantially higher frequencies compared to *R. pipiens*.

Further research related to the electrical properties of the AP hair cells may afford added insight into their frequency responses along the organ's tonotopic axis. While BP tuning is hypothesized to be mechanical in origin, there is electrical tuning in low-frequency AP hair cells (Pitchford and Ashmore, 1987; Smotherman and Narins, 1999b, 2000). Furthermore, ion channel kinetics have been demonstrated to change by an order of magnitude along the tonotopic axis of the *R. pipiens* AP (Smotherman and Narins, 1999b, 2000). Electrical tuning properties and ion channel compositions that differ between species' AP hair cells may complement mechanical tuning mechanisms to differentiate further the frequency response properties of the ultrasound-sensitive frogs and *R. pipiens* APs.

4.4. Lao torrent frogs

Currently, very little is known about the life histories of *O. chloronota* and *A. daorum*, including their acoustic communication systems. However, we hypothesized that they are candidates for the use of high-frequency/ultrasonic communication because they are found in sympatry alongside rushing montane streams that produce high-level, predominately low-frequency ambient noise that closely matches the noise in the environments of *H. cavitympanum*, *O. tormota* and *O. livida* (Arch and Narins, personal obs.; Feng et al., 2006; Arch et al., 2008; Arch and Narins, 2008).

We found that the morphometrics of the *O. chloronota* auditory organs are remarkably convergent with those of the ultrasonically sensitive frogs, and are statistically indistinguishable from *H. cavitympanum* in every morphological feature measured (Figs. 3 and 5). As a result, we suggest that this species is a strong candidate for high-frequency/ultrasonic hearing. By contrast, the statistical results for *A. daorum* were generally intermediate between the ultrasound-detecting species and *R. pipiens*. The power of these tests, however, was significantly reduced by our small sample size. Based on the trends in the data, it appears that the auditory morphology of *A. daorum* is different from the ultrasonically sensitive frogs in every metric for which there was a group difference among the species (Figs. 3 and 5). Interestingly, *A. daorum* SL and BL were comparable to those of *R. pipiens* in both auditory organs, despite the fact that *A. daorum* and *R. pipiens* are the smallest and largest of the species examined, respectively [SVL: 36 mm (Bain et al., 2003) versus 63.5 mm (Arch, personal obs.)]. These results imply that SL and BL values are decoupled from body size. This conclusion is consistent with our hypothesis that these are key morphological features influencing high-frequency sensitivity; to date, ultrasonic hearing ability does not appear to relate directly with body size [e.g., *H. cavitympanum* avg. SVL = 45 mm (Yang, 1991); *O. tormota* avg. SVL = 34 mm (Fei, 1999); *O. livida* avg. SVL = 48 mm (Fei, 1999)]. Based on our data from *A. daorum*, we conclude that this species is unlikely to detect ultrasound. Future experiments employing electrophysiological recording from the auditory midbrain and/or VIIIth nerve of the Lao species will help determine whether auditory morphology can be used to predict the extent of high-frequency hearing.

5. Conclusion

Our comparison of the morphological features of the *H. cavitympanum*, *O. tormota*, *O. livida* and *R. pipiens* inner ears is a first step toward understanding the structural and physiological mechanisms that enable high-frequency detection in frogs. A striking inner-ear morphological convergence occurs among species from two distantly related genera. From these data, we postulate that relatively small-scale adjustments in morphological features related to the mass and stiffness of the resonance systems within the auditory organs play key roles in facilitating high-frequency

transduction. Accordingly, we propose that the acquisition of ultrasonic hearing evolved through gradual and convergent modifications of the frog ear, rather than through a major reorganization of the transduction apparatus. Subsequent experimental work will be necessary to determine causal relationships between our morphological observations and high-frequency transduction ability. Exploring the frequency sensitivity of *O. chloronota* provides an excellent opportunity to begin this work, since the species' ear morphology is remarkably convergent with that of the demonstrated ultrasound-sensitive species. These ongoing investigations will continue to elucidate the peripheral mechanisms enabling a non-mammalian vertebrate to transduce extraordinarily high frequencies.

Acknowledgments

We are grateful to Dr. Larry Hoffman (UCLA, Department of Head and Neck Surgery) for providing advice, resources and time during the initial stages of this research project. We thank Aubrey Hawkes for substantial assistance with methodological development and Dr. Stephen Arch for helpful comments on the manuscript.

Appendix. Supplementary data

Supplementary data related to this article can be found online at doi:10.1016/j.heares.2011.11.006.

References

Arch, V.S., Grafe, T.U., Gridi-Papp, M., Narins, P.M., 2009. Pure ultrasonic communication in an endemic Bornean frog. PLoS ONE 4, e5413.
Arch, V.S., Grafe, T.U., Narins, P.M., 2008. Ultrasonic signalling by a Bornean frog. Biol. Lett. 4, 19–22.
Arch, V.S., Narins, P.M., 2008. 'Silent' signals: selective forces acting on ultrasonic communication systems in terrestrial vertebrates. Anim. Behav. 76, 1423–1428.
Authier, S., Manley, G.A., 1995. A model of frequency tuning in the basilar papilla of the Tokay gecko, *Gekko gecko*. Hear. Res. 82, 1–13.
Bain, R., Lathrop, A., Murphy, R.W., Orlov, N.L., Cuc, H.T., 2003. Cryptic species of a cascade frog from Southeast Asia: taxonomic revisions and descriptions of six new species. Amer. Mus. Nov. 3417, 1–60.
Baird, I.L., 1974. Some aspects of the comparative anatomy and evolution of the inner ear in submammalian vertebrates. Brain Behav. Evol. 10, 11–36.
Bohne, B.A., Carr, C.D., 1985. Morphometric analysis of hair cells in the chinchilla cochlea. J. Acoust. Soc. Am. 77, 153–158.
Capranica, R.R., 1976. Morphology and physiology of the auditory system. In: Llinas, R., Precht, W. (Eds.), Frog Neurobiology. Springer-Verlag, Berlin, pp. 551–575.
Capranica, R.R., Moffat, A.J.M., 1977. Place mechanism underlying frequency analysis in the toad's inner ear. J. Acoust. Soc. Am. 6, S36.
Dooling, R.J., Lohr, B., Dent, M.L., 2000. Hearing in birds and reptiles. In: Dooling, R.J., Fay, R.R., Popper, A.N. (Eds.), Comparative Hearing: Birds and Reptiles. Springer, New York, pp. 308–360.
Echteler, S.M., Fay, R.R., Popper, A.N., 1994. Structure of the mammalian cochlea. In: Fay, R.R., Popper, A.N. (Eds.), Comparative Hearing: Mammals. Springer, New York, pp. 134–171.
Fei, L., 1999. Atlas of Amphibians of China. Zhengzhou: Henan Science and Technology Press.
Feng, A.S., Narins, P.M., Capranica, R.R., 1975. Three populations of primary auditory fibers in bullfrog (*Rana catesbeiana*) - their peripheral origins and frequency sensitivities. J. Comp. Physiol. 100, 221–229.
Feng, A.S., Narins, P.M., Xu, C.-H., 2002. Vocal acrobatics in a Chinese frog, *Amolops tormotus*. Naturwissen 89, 352–356.
Feng, A.S., Narins, P.M., Xu, C.-H., Lin, W.-Y., Yu, Z.-L., Qiu, Q., Xu, Z.-M., Shen, J.-X., 2006. Ultrasonic communication in frogs. Nature 440, 333–336.
Feng, A.S., Shofner, W.P., 1981. Peripheral basis of sound localization in anurans. Acoustic properties of the frog's ear. Hear. Res. 5, 201–216.
Fettiplace, R., Fuchs, P.A., 1999. Mechanisms of hair cell tuning. Ann. Rev. Physiol. 61, 809–834.
Flock, A., 1977. Physiological properties of sensory hairs in the ear. In: Evans, E.F., Wilson, J.P. (Eds.), Psychophysics and Physiology of Hearing. Academic Press, London, pp. 15–25.
Flock, A., 1982. Structure and function of the hearing organ: recent investigations of micromechanics and its control. In: Carlson, R., Granstrom, B. (Eds.), The Representation of Speech in the Peripheral Auditory System. Elsevier, Amsterdam, pp. 1–8.
Fuchs, P.A., Nagai, T., Evans, M.G., 1988. Electrical tuning in hair cells isolated from the chick cochlea. J. Neurosci. 8, 2460–2467.
Geisler, C.D., Van Bergeijk, W.A., Frishkopf, L.S., 1964. The inner ear of the bullfrog. J. Morph 114, 43–57.
Gridi-Papp, M., Feng, A.S., Shen, J.-X., Yu, Z.-L., Rosowski, J.J., Narins, P.M., 2008. Active control of ultrasonic hearing in frogs. Proc. Nat. Acad. Sci. USA 105, 11014–11019.
Hackney, C.M., Fettiplace, R., Furness, D.N., 1993. The functional morphology of stereociliary bundles on turtle cochlear hair cells. Hear. Res. 69, 163–175.
Heffner, H.E., Heffner, R.S., 1998. Hearing. In: Greenberg, G., Haraway, M.M. (Eds.), Comparative Psychology: a Handbook. Routledge, New York, pp. 290–303.
Heffner, H.E., Heffner, R.S., 2007. High-frequency hearing. In: Basbaum, A., Bushnell, M., Smith, D., Beauchamp, G., Firestein, S., Dallos, P., Oertel, D., Masland, R., Albright, T., Kaas, J. (Eds.), The Senses: a Comprehensive Reference. Academic Press, St. Louis, pp. 55–60.
Hillery, C.M., Narins, P.M., 1984. Neurophysiological evidence for a traveling wave in the amphibian inner ear. Science 4666, 1037–1039.
Hillery, C.M., Narins, P.M., 1987. Frequency and time domain comparison of low-frequency auditory fiber responses in two anuran amphibians. Hear. Res. 25, 233–248.
Iurato, S., 1967. Submicroscopic Structure of the Inner Ear. Pergamon, Oxford.
Köppl, C., Authier, S., 1995. Quantitative anatomical basis for a model of micromechanical frequency tuning in the Tokay gecko, *Gekko gecko*. Hear. Res. 82, 14–25.
Lewis, E.R., 1976. Surface morphology of the bullfrog amphibian papilla. Brain Behav. Evol. 13, 196–215.
Lewis, E.R., Baird, R., Leverenz, E.L., Koyama, H., 1982a. Inner ear: dye injection reveals peripheral origins of specific sensitivities. Science 215, 1641–1643.
Lewis, E.R., Hecht, E.I., Narins, P.M., 1992. Diversity of form in the amphibian papilla of Puerto Rican frogs. J. Comp. Physiol. A 17, 421–435.
Lewis, E.R., Leverenz, E.L., 1983. Morphological basis for tonotopy in the anuran amphibian papilla. Scan. Elect. Micro 1983, 189–200.
Lewis, E.R., Leverenz, E.L., Koyama, H., 1982b. The tonotopic organization of the bullfrog amphibian papilla, an auditory organ lacking a basilar membrane. J. Comp. Physiol. A 145, 437–445.
Lewis, E.R., Li, C.W., 1975. Hair cell types and distributions in the otolithic and auditory organs of the bullfrog. Brain Res. 83, 35–50.
Lim, D.J., 1980. Cochlear anatomy related to cochlear micromechanics. A review. J. Acoust. Soc. Am. 67, 1686–1695.
Loftus-Hills, J.J., Johnstone, B.M., 1970. Auditory function, communication, and the brain-evoked response in anuran amphibians. J. Acoust. Soc. Am. 47, 1131–1138.
Lombard, R.E., Bolt, J.R., 1979. Evolution of the tetrapod ear: an analysis and reinterpretation. Biol. J. Linn. Soc. 11, 19–76.
Mann, D.A., Higgs, D.M., Tavolga, W.N., Souza, M.J., Popper, A.N., 2001. Ultrasound detection by clupeiform fishes. J. Acoust. Soc. Am. 109, 3048–3054.
Meenderink, S.W.F., van Dijk, P., Narins, P.M., 2005. Comparison between distortion product otoacoustic emissions and nerve fiber responses from the basilar papilla of the frog. J. Acoust. Soc. Am. 117, 3165–3173.
Megela, A.L., Capranica, R.R., 1982. Differential patterns of physiological masking in the anuran auditory nerve. J. Acoust. Soc. Am. 71, 641–645.
Mulroy, M.J., 1974. Cochlear anatomy of the alligator lizard. Brain Behav. Evol. 10, 69–87.
Narins, P.M., 1990. Seismic communication in anuran amphibians. Bioscience 40, 268–274.
Narins, P.M., Feng, A.S., Lin, W.-Y., Schnitzler, H.Ü., Denzinger, A., Xu, C.-H., 2004. Old World frog and bird vocalizations contain prominent ultrasonic harmonics. J. Acoust. Soc. Am. 115, 910–913.
Narins, P.M., Hillery, C.M., 1983. Frequency coding in the inner ear of anuran amphibians. In: Klinke, R., Hartmann, R. (Eds.), Hearing- Physiological Bases and Psychophysics. Springer-Verlag, Heidelberg, pp. 70–76.
Pitchford, S., Ashmore, J., 1987. An electrical resonance in hair cells of the amphibian papilla of *Rana temporaria*. Hear. Res. 27, 75–83.
Purgue, A.P., Narins, P.M., 2000a. Mechanics of the inner ear of the bullfrog (*Rana catesbeiana*): the contact membranes and the periotic canal. J. Comp. Physiol. A 186, 481–488.
Purgue, A.P., Narins, P.M., 2000b. A model for energy flow in the inner ear of the bullfrog (*Rana catesbeiana*). J. Comp. Physiol. A 186, 489–495.
R Development Core Team., 2004. R: R Foundation for Statistical Computing (Vienna, Austria).
Ronken, D.A., 1990. Basic properties of auditory-nerve responses from a "simple" ear: the basilar papilla of the frog. Hear. Res. 47, 63–82.
Schoffelen, R., Segenhout, J., van Dijk, P., 2009. Tuning of the tectorial membrane in the basilar papilla of the Northern Leopard frog. J. Assoc. Res. Otolaryngol. 10, 309–320.
Shofner, W.P., Feng, A.S., 1981. Post-metamorphic development of the frequency selectivities and sensitivities of the peripheral auditory system of the bullfrog, *Rana catesbeiana*. J. Exp. Biol. 93, 181–196.
Shofner, W.P., Feng, A.S., 1983. A quantitative light microscopic study of the bullfrog amphibian papilla tectorium: correlation with the tonotopic organization. Hear. Res. 11, 103–116.
Shofner, W.P., Feng, A.S., 1984. Quantitative light and scanning electron-microscopic study of the developing auditory organs in the bullfrog: Implications on their functional characteristics. J. Comp. Neurol. 224, 141–154.

Simmons, D.D., Bertolotto, C., Narins, P.M., 1994. Morphological gradients in sensory hair cells of the amphibian papilla of the frog, *Rana pipiens pipiens*. Hear. Res. 80, 71–78.

Smotherman, M.S., Narins, P.M., 1998. Effect of temperature on electrical resonance in leopard frog saccular hair cells. J. Neurophysiol. 79, 312–321.

Smotherman, M.S., Narins, P.M., 1999a. Potassium currents in auditory hair cells of the frog basilar papilla. Hear. Res. 132, 117–130.

Smotherman, M.S., Narins, P.M., 1999b. The electrical properties of auditory hair cells in the frog amphibian papilla. J. Neurosci. 19, 5275–5292.

Smotherman, M.S., Narins, P.M., 2000. Hair cells, hearing and hopping: a field guide to hair cell physiology in the frog. J. Exp. Biol. 203, 2237–2246.

Strelioff, D., Flock, A., 1982. Mfechanical properties of hair bundles of receptor cells in the guinea pig cochlea. Soc. Neurosci. Abs 8, 40.

Stuart, B.L., 2008. The phylogenetic problem of *Huia* (Amphibia: Ranidae). Mol. Phylo. Evol. 46, 49–60.

Sugihara, I., Furukawa, T., 1989. Morphological and functional aspects of two different types of hair cells in the goldfish sacculus. J. Neurophysiol. 62, 1330–1343.

Tilney, L., Saunders, J., 1983. Actin filaments, stereocilia, and hair cells of the bird cochlea. I. Length, number, width, and distribution of stereocilia of each hair cell are related to the position of the hair cell on the cochlea. J. Cell Biol. 96, 807–821.

Turner, R.G., Muraski, A.A., Nielsen, D.W., 1981. Cilium length: influence on neural tonotopic organization. Science 213, 1519–1521.

van Dijk, P., Manley, G., 2001. Distortion product otoacoustic emissions in the tree frog *Hyla cinerea*. Hear. Res. 153, 14–22.

van Dijk, P., Meenderink, S., 2006. Distortion product otoacoustic emissions in the amphibian ear. In: Nuttall, A.L., Renn, T., Gillespie, P., Grosh, K., deBoer, E. (Eds.), Auditory Mechanisms, Processes and Models. World Scientific, Singapore, pp. 332–338.

Wada, T., 1923. Anatomical and physiological studies on the growth of the inner ear of the albino rat. In: Huntington, G.S., Stockard, C.R., Evan, H.M. (Eds.), The American Anatomical Memoirs. The Wistar Institute of Anatomy and Biology, Philadelphia, pp. 1–174.

Wever, E.G., 1985. The Amphibian Ear. Princeton University Press, Princeton.

Wever, E.G., 1973. The ear and hearing in the frog, *Rana pipiens*. J. Morph 141, 461–477.

Wilczynski, W., Capranica, R.R., 1984. The auditory system of anuran amphibians. Prog. Neurobiol. 22, 1–38.

Yang, D., 1991. Phylogenetic systematics of the *Amolops* group of ranid frogs of southeastern Asia and the Greater Sunda Islands. Field Zool. New Ser. 63, 1–42.

Yu, X., Lewis, E.R., Feld, D., 1991. Seismic and auditory tuning curves from bullfrog saccular and amphibian papillar axons. J. Comp. Physiol. A 169, 241–248.

Zwislocki, J.J., 1980a. Five decades of research on cochlear mechanics. J. Acoust. Soc. Am. 67, 1679–1685.

Zwislocki, J.J., 1980b. Theory of cochlear mechanics. Hear. Res. 2, 171–182.